Sensitive Elements for Wirelessly Interrogated High Temperature SAW Deformation Sensors

A. Shvetsov, S. Zhgoon, A. Merkulov, N. Belyankin
Department of Radio Engineering Fundamentals
National Research University "MPEI"
Moscow, Russia
shvetsov_as@mail.ru

P.W. Mengue, O. Elmazria
Institut Jean Lamour UMR 7198
Université de Lorraine - CNRS
Nancy, France
omar.elmazria@univ-lorraine.fr

***Abstract*—The surface acoustic waves (SAW) delay sensitivity to different types of deformation was calculated for different orientations of langasite (LGS) substrate. Besides LGS properties recent experimental data from several sources related to high-temperature SAW sensors are discussed that also show useful properties of other materials. Notably catangasite (CTGS) is a promising candidate for replacing LGS. The applicability of devices based on lithium niobate (LN) was obtained up to 600°C paving the way to wide-bandwidth devices. For mounting the deformation sensors onto DUT testing of different high-temperature adhesives was carried out. Another way to high-temperature deformation sensor development makes use of piezoelectric thin film directly deposited on a metallic object whose deformation is measured. Successful testing of ZnO/metal-based devices is appealing, because the direct deposition of piezoelectric layer on metal can allow to directly measure the strain of the monitored object and thus to eliminate the hysteresis and unreliable strain transfer in a wide range of temperatures.**

Keywords—wireless sensor; passive sensor; SAW sensor; high temperature; deformation measurement

I. Introduction

Deformation measurement including measurement at elevated temperatures is important for airspace, structural health monitoring, power engineering. SAW sensors are especially interesting as sensitive elements of passive (batteryless) sensors that can be remotely (wirelessly) interrogated by electromagnetic waves. Particular properties of SAW devices allow them to work in extremely harsh environment including high temperature up to several hundred degrees Celsius. Applications of high-temperature SAW sensors are well-known [1]. The measurements of mechanical values based on measurements of strain at normal condition are also well-known [2]. The measurements of mechanical values at elevated temperatures by SAW sensors were recently discussed [3]. At high temperatures technical problems with measurements of mechanical values become more complicated. The choice of electrode materials, the choice of piezoelectric single crystal substrates and of sensor to object bonding technique or the choice of thin film piezoelectric layer [4] are significant for solving of these problems.

Sensitivity to selected mechanical impacts was studied for a restricted variety of LGS orientations [5 – 8]. Here the sensitivity to deformation was calculated for SAW with lowest velocity for all possible orientations of LGS substrate. The sensitivities to all independent components of arbitrary deformation in substrate plane were calculated. The SAW devices on different substrates with different electrode materials that were tested at elevated temperatures [9 – 15] are compared. Different methods of single crystal sensor bonding to the object subjected to strain were tested. Single crystal SAW sensors are compared with those based on ZnO thin films directly deposited on a metallic object whose deformation is measured.

II. Brief Review of Piezoelectric Substrate Materials

LGS ($La_3Ga_5SiO_{14}$) is the most studied material among SAW device substrates for high temperature application. Many recent publications report stable operation of LGS-based devices at high temperature: 384 hours at 600°C [9]; 300 hours at 843°C [10]; 160 hours at 1050°C and 130 hours at 1100°C [11]; 1140°C was reached in [12]. Different results are caused by different electrode structures that are currently intensively investigated especially on LGS substrates. CTGS ($Ca_3TaGa_3Si_2O_{14}$) is a promising candidate for replacing LGS because it has an ordered structure resulting in better properties at elevated temperatures [13]. LN ($LiNbO_3$) is interesting because of the high electromechanical coupling. Stoichiometric LN (SLN) is preferable for high temperature application in comparison to congruent LN [14], SLN-based SAW device was successfully tested up to 600°C [15]. A variety of other materials exists and it is described in recent detailed reviews [16, 17].

III. Single Crystal Strain Sensor Mounting

The choice of appropriative adhesive is significant for strain measuring. Even at 100°C adhesive properties can result in hysteresis, creep and strain transfer reduction [18, 19]. Sensor mounting becomes a more complicated task with working temperature increase. Organic adhesives will fail with every next requirement to further increase the temperature. In order to move in this direction inorganic materials are necessary. Tests of several such materials were reported:

The investigation was carried out within the framework of the project "Wireless passive fast-varying deformation sensors" with the support of a grant from NRU "MPEI" for implementation of scientific research programs "Energy", "Electronics, Radio Engineering and IT" , and "Industry 4.0, Technologies for Industry and Robotics in 2020-2022".

978-1-6654-3935-0/21/$31.00 ©2021 IEEE

"Al_2O_3 ceramic high temperature epoxy" up to 120 με at 400°C (up to 200 με at 24°C) [20]; "inorganic adhesive (OMEGABOND 500)" up to 700 με at 250°C [21]. Also, metallic materials (in particular NanoFoil [22]) or glass-like materials (such as borosilicate glass [23] and glass frit [24]) can be used.

Our initial experiments on sensor mounting were carried out with dielectric paste (DP) and conductive paste (CP) used in outdated hybrid integrated circuits manufacturing. CP allows to create a thin robust layer with good adhesion by heating up to 550 - 600°C, thicker layer after annealing has a porous structure and does not achieve a sufficient strength after such moderate heating. DP forms a ceramic-like layer independently on its thickness, but it is not robust after moderate heating too. Heating to higher temperature (about 900°C) increases the layer strength in most cases, but it is appropriate only to sensors withstanding such heating, besides the problem of thermal expansion mismatch becomes more serious.

IV. Calculation Method

Following the approach described in [25] the influence of the static deformation on small-amplitude elastic wave is taken into account by the transformation of initial elastic constants C into perturbed elastic constants A by

$$A_{ijkl} = C_{ijkl} + C_{ipkl}\frac{\partial U_j}{\partial x_p} + C_{ijql}\frac{\partial U_k}{\partial x_q} + C_{ijkluv}S_{uv} + \delta_{jk}T_{il} \quad (1)$$

where U, S, and T are static displacement, strain, and stress respectively. We carried out the calculation by a modified freeware software VCAL [26]. LGS second order material constants from [27] were used for this calculation. The third order LGS elastic constants [28] are available for room temperature only, so the calculation results can be used only for the initial choice of substrate orientation intended for high temperature application.

Using perturbed elastic constants depending on S in equation of motion and boundary conditions we can calculate SAW velocity V depending on S. Note that (1) is compatible with equations of motion and boundary conditions referred to initial coordinate system. It means that V is related to the initial length but not to the perturbed length, thus the SAW time-delay τ sensitivity to strain

$$(\partial\tau / \partial S) / \tau = -(\partial V / \partial S) / V \quad (2)$$

and the length change does not need to be additionally accounted for. Correspondingly the SAW resonator frequency f_r sensitivity to strain (without taking into account the influence of electrode structure)

$$(\partial f_r / \partial S) / f_r \approx -(\partial\tau / \partial S) / \tau = (\partial V / \partial S) / V. \quad (3)$$

V. Calculation Results

In order to comply with LGS symmetry the calculation in the following range of Euler angles is sufficient: first angle φ from 0 to 30º, second angle θ from 0 to 180º, third angle ψ from 0 to 180º. Calculation results are illustrated in contour maps for SAW time-delay sensitivity which are shown in Fig. 1 – 5. Each figure contains a pair of maps corresponding to the values of the first Euler angle 0 and 30°.

Fig. 1 – 3 show the sensitivity to three basic independent in-plane strain components. Fig. 4, 5 show the sensitivity to other main in-plane deformations. One can determine the sensitivity of τ or f_r to arbitrary mechanical impact producing strain predominantly in substrate plane by data from these figures after calculation of three independent basic strain components which accompany this mechanical impact.

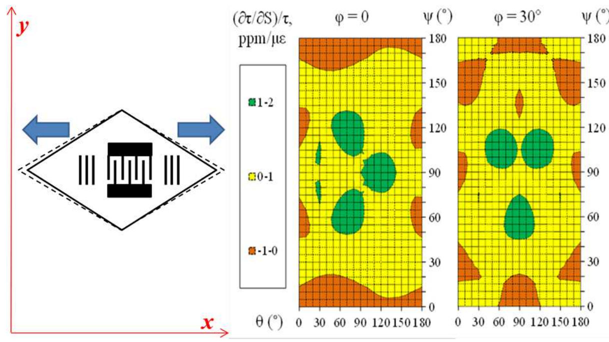

Fig. 1. Dependence of SAW time-delay sensitivity to uniaxial tensile-compressive deformation along the SAW propagation direction ($S = S_{xx}$, $S_{yy} = S_{xy} = S_{yx} = 0$, a visual explanation is on the left of the figure) on LGS substrate orientation.

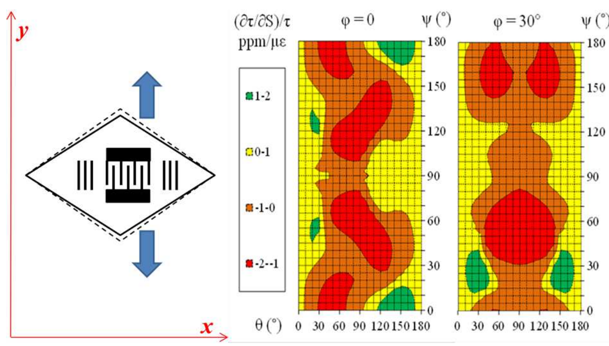

Fig. 2. Dependence of SAW time-delay sensitivity to uniaxial tensile-compressive deformation along the electrodes ($S = S_{yy}$, $S_{xx} = S_{xy} = S_{yx} = 0$, a visual explanation is on the left of the figure) on LGS substrate orientation.

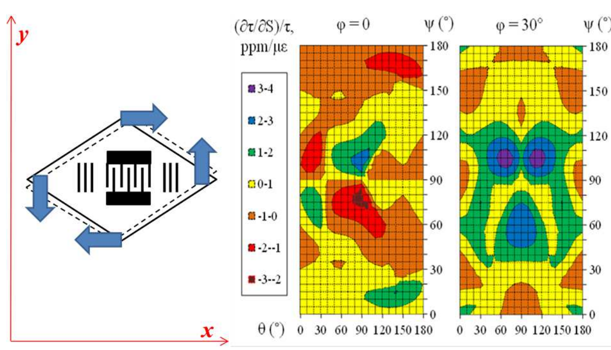

Fig. 3. Dependence of SAW time-delay sensitivity to shear deformation along the SAW propagation direction and/or along the electrodes ($S = S_{xy} = S_{yx}$, $S_{xx} = S_{yy} = 0$, a visual explanation is on the left of the figure) on LGS substrate orientation.

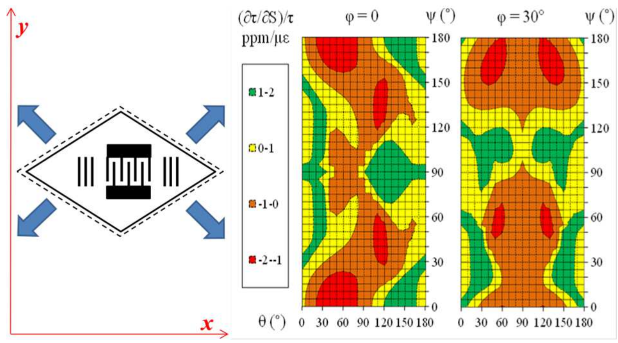

Fig. 4. Dependence of SAW time-delay sensitivity to all-round in-plane tensile-compressive deformation ($S = S_{xx} = S_{yy}$, $S_{xy} = S_{yx} = 0$, a visual explanation is on the left of the figure) on LGS substrate orientation.

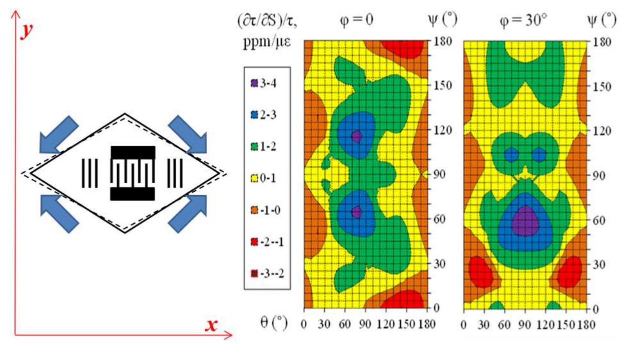

Fig. 5. Dependence of SAW time-delay sensitivity to tensile-compressive deformation along the SAW propagation direction with compressive-tensile deformation along the electrodes ($S = S_{xx} = -S_{yy}$, $S_{xy} = S_{yx} = 0$, a visual explanation is on the left of the figure) on LGS substrate orientation.

The maps indicate regions with LGS substrate orientations that provide the greatest values of deformation sensitivity (at least at room temperature). These regions are marked by cherry, blue, and violet (Fig. 3 and 5). Substrate orientations with sensitivity values closer to local extrema are summarized in Table I together with values of electromechanical coupling factor K^2 and power flow angle (PFA).

TABLE I. CHARACTERISTICS OF SAW FOR SELECTED SUBSTRATE ORIENTATIONS

Substrate orientation (Euler angles)	**SAW time-delay sensitivity (ppm/με) to strain *S* = ...**					**K^2**	**PFA**
	S_{xx}	S_{yy}	$S_{xx} = S_{yy}$	$S_{xy} = S_{yx}$	$S_{xx} = -S_{yy}$		
30°, 90°, 60°	1.5	-2	-0.5	3	3.5	0.007	16°
30°, 70°, 105°	1.7	-0.5	1.2	3.4	2.2	0.07	11°
30°, 30°, 35°	0.5	1.3	1.8	0.9	-0.9	0.016	23°
0, 50°, 0	-0.4	-1.4	-1.8	0	0.9	0.16	0
0, 120°, 90°	1.6	0.1	1.8	0	1.5	0.004	0
0, 140°, 0	-0.2	1.9	1.7	0	-2.1	0.004	0
0, 80°, 65°	1.6	-1.5	0.05	-1.2	3.1	0.03	15°
0, 90°, 80°	0.8	-1	-0.2	-2.4	1.8	0.02	7°
0, 140°, 15°	0.5	0.9	1.4	2.1	-0.4	0.08	5°

VI. SENSORS BASED ON PIEZOELECTRIC THIN FILMS

Another way to mounting the strain sensor is the direct deposition of piezoelectric thin film (AlN and ZnO are the most used materials for this purpose) over the object subjected to deformation. Such objects are metallic in most examples of practical applications. Test of AlN/TC4-alloy-based SAW device up to 400 με at 400°C was reported [29], while AlN itself has been shown to withstand 1050°C [30]. The characteristics of such sensors strongly depend on the material of the monitored object, thus, experiments with different useful metals and alloys are very important. A test of ZnO/Titanium-based SAW device [4] temperature behavior is presented here (Fig. 6, 7). The Q-factor of this SAW resonator is about 413, the relative difference of antiresonance and resonance frequencies is about 0.48% and the factor of merit is about 2. Fig. 7 shows that the resonator retains workability up to 400°C.

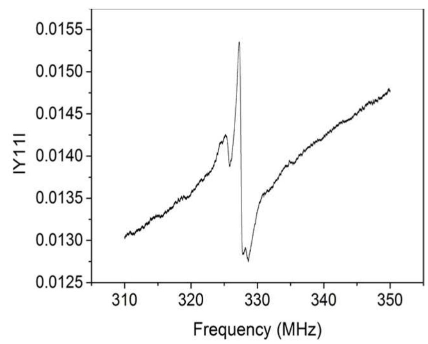

Fig. 6. The frequency dependence of the admittance absolute value of the ZnO/Ti SAW resonator.

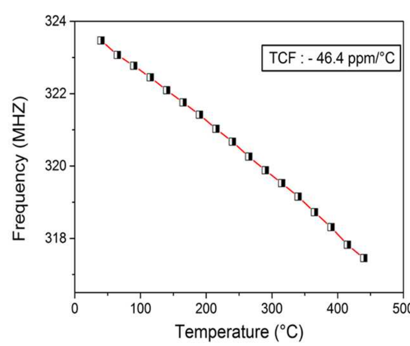

Fig. 7. The temperature dependence of the resonance frequency of the ZnO/Ti SAW resonator.

VII. DISCUSSION

The shear deformations allow to achieve larger sensitivity to strain than tensile-compressive deformations. The largest sensitivity does not accompany reasonable values of K^2 and PFA, consequently, the search of trade-off between sensitivity to strain and other relevant parameters is necessary. An example of orientation with compromise properties is the orientation with Euler angles (0, 50°, 0).

Advantages of single crystal sensors are: a more developed SAW device fabrication technique, a possibility of sensor bonding to locations that do not allow thin film deposition, and preserving of main characteristics independently on material of the monitored object. Their disadvantage is the necessity of an adhesive that restricts reliable strain transfer especially with increasing of the working temperature. Overcoming of this problem is the advantage of piezoelectric thin film sensors.

VIII. Conclusions

Single crystal sensors have some advantages but present difficulties with their bonding to object that restrict their application, thus, further investigation of sensor bonding methods is required. LGS orientation with maximal sensitivity to in-plane strain are determined, this data can be useful for sensor designers. Successful testing of piezoelectric thin film/metal-based devices is appealing, because the direct deposition of piezoelectric layer on metal can allow to directly measure the strain of the monitored object and to eliminate the hysteresis and unreliable strain transfer in a wide temperature range. Both approaches are interesting for further development and application.

Acknowledgment

The use of Ken-ya Hashimoto software is gratefully acknowledged.

References

[1] P. Zheng, D. W. Greve, I. J. Oppenheim, and V. Malone, "Langasite SAW temperature and oxygen multi-sensor", Joint Conference of the IEEE International Frequency Control and the European Frequency and Time Forum (FCS) Proceedings, pp. 1–4, 2011.

[2] V. Kalinin, "Wireless physical SAW sensors for automotive applications", IEEE International Ultrasonics Symposium, 2011, pp. 212–221, 2011.

[3] A. Maskay and M. Pereira da Cunha, "High-temperature microwave acoustic vibration sensor", IEEE International Ultrasonics Symposium, pp. 1–3, 2018.

[4] P. Mengue, S. Hage-Ali, O. Elmazria, and S. Zhgoon, "SAW sensors directly integrated onto industrial metallic parts for manufacturing 4.0", IEEE International Workshop on Metrology for Industry 4.0 & IoT, pp. 158–161, 2020.

[5] R. M. Taziev, "Stress, temperature and pressure behavior of SAW on langasite plates," Proceedings of the 2001 IEEE International Frequncy Control Symposium and PDA Exhibition, pp. 227–234, 2001.

[6] G. Bruckner, G. Stampf, G. Franz, R. Fachberger, and R. Hauser, "SAW strain sensitivity of selected Rayleigh wave crystal cuts,' IEEE International Ultrasonics Symposium, pp. 823–826, 2009.

[7] H. Zhang and J. A. Kosinski, "Analysis of contributions of nonlinear material constants to stress-induced velocity shifts of quartz and langasite surface acoustic wave resonators," IEEE Transactions on Ultrasonics, Ferroelectrics, and Frequency Control, vol. 60, no. 5, pp. 975–985, May 2013.

[8] F. Cai et al., "Sensitivity analysis of langasite surface acoustic wave pressure sensors," Symposium on Piezoelectricity, Acoustic Waves, and Device Applications (SPAWDA), pp. 77–80, 2017.

[9] A. De Sousa Lopes Moreira, L. Arapan, and A. Bartasyte, "New approach of interdigitated transducers engineering for high-temperature surface acoustic wave sensors," IEEE International Ultrasonics Symposium (IUS), 2020, pp. 1–4.

[10] A. Ayes, G. Bernhardt, and M. P. da Cunha, "Removal of stress hillocks from platinum-alumina electrodes used in high-temperature SAW devices," IEEE International Ultrasonics Symposium (IUS), pp. 727–730, 2019.

[11] R. Behanan et al., "Thin films and techniques for SAW sensor operation above 1000°C," IEEE International Ultrasonics Symposium (IUS), pp. 1013–1016, 2013.

[12] T. Aubert, O. Elmazria, J. Bardong, and G. Bruckner, "Iridium interdigital transducers for ultra-high-temperature SAW devices," IEEE International Ultrasonics Symposium, pp. 2065–2068, 2011.

[13] A. Sotnikov et al., "Material parameters of $Ca_3TaGa_3Si_2O_{14}$ (CTGS) piezoelectric single crystal at extreme temperatures," Joint Conference of the European Frequency and Time Forum and IEEE International Frequency Control Symposium (EFTF/IFCS), pp. 193–197, 2017.

[14] Y. Li et al., "The high temperature resistivity of lithium niobate and related crystals," Proceedings of the 2014 Symposium on Piezoelectricity, Acoustic Waves, and Device Applications, pp. 283–286, 2014.

[15] T. Aubert et al., "First investigations on stoichiometric lithium niobate as piezoelectric substrate for high-temperature surface acoustic waves applications," IEEE Sensors, pp. 1–3, 2017.

[16] H. Zu, H. Wu, and Q. Wang, "High-Temperature Piezoelectric Crystals for Acoustic Wave Sensor Applications," IEEE Transactions on Ultrasonics, Ferroelectrics, and Frequency Control, vol. 63, no. 3, pp. 486–505, March 2016.

[17] F. Yu et al., "High temperature piezoelectric single crystals: recent developments," Symposium on Piezoelectricity, Acoustic Waves, and Device Applications (SPAWDA), pp. 1–7, 2016.

[18] V. Kalinin, "Modelling of hysteresis and creep in SAW strain sensors," IEEE International Frequency Control Symposium (FCS), pp. 1–4, 2014.

[19] V. Kalinin, A. Leigh, A. Nowell, and C. Pilgrim, "Strain transfer and creep in all-quartz packaged SAW strain sensors," IEEE International Frequency Control Symposium (IFCS), pp. 1–6, 2018.

[20] A. Maskay and M. Pereira da Cunha, "High temperature static strain microwave acoustic sensor," IEEE International Ultrasonics Symposium (IUS), pp. 1–4, 2016.

[21] L. Li et al., "Strain measurements with langasite SAW resonators at high temperature," IEEE Sensors Journal, vol. 21, no. 4, pp. 4688–4695, February 2021.

[22] P. Nicolay, J. Bardong, H. Chambon, and P. Dufilié, "Glue-Less and robust assembly method for SAW strain sensors," IEEE International Ultrasonics Symposium (IUS), pp. 1–4, 2018.

[23] N. Subbiah, S. Ghosh, J. Wilde, and R. Zeiser, "Comparison of packaging concepts for high-temperature pressure sensors at 500 °C," IEEE 67th Electronic Components and Technology Conference (ECTC), pp. 949–955, 2017.

[24] S. Ballandras et al., "Micro-machined, all quartz package, passive wireless SAW pressure and temperature sensor," IEEE Ultrasonics Symposium, pp. 1441–1444, 2006.

[25] J. J. Gagnepain, "Nonlinear constants and their significance," 41st Annual Symposium on Frequency Control, pp. 266–276, 1987.

[26] K. Hashimoto and M. Yamaguchi, "Free software products for simulation and design of surface acoustic wave and surface transverse wave devices," Proceedings of 1996 IEEE International Frequency Control Symposium, pp. 300–306, 1996.

[27] S. Sakharov, P. Senushencov, A. Medvedev, and Y. Pisarevsky, "New data on temperature stability and acoustical losses of langasite crystals," Proceedings of the 1995 IEEE International Frequency Control Symposium (49th Annual Symposium), pp. 647–652, 1995.

[28] B. P. Sorokin, P. P. Turchin, S. I. Burkov, D. A. Glushkov, and K. S. Aleksandrov, "Influence of static electric field, mechanical pressure and temperature on the propagation of acoustic waves in $La_3Ga_5SiO_{14}$ piezoelectric single crystals," Proceedings of 1996 IEEE International Frequency Control Symposium, pp. 161–169, 1996.

[29] L. Shu et al., "The investigation of integrated SAW strain sensor based on AlN/TC4 structure," Sensors and Actuators A: Physical, vol. 293, pp. 14–20, April 2019.

[30] T. Aubert, O. Elmazria, J. Bardong, G. Bruckner, and B. Assouar, "Is AlN/Sapphire bilayer structure an alternative to langasite for ultra-high-temperature SAW applications?," IEEE International Ultrasonics Symposium, pp. 2082–2085, 2011.